

See discussions, stats, and author profiles for this publication at: <https://www.researchgate.net/publication/260269359>

Small Molecule-Initiated Light-Activated Semiconducting Polymer Dots: An Integrated Nanoplatform for Targeted Photodynamic Therapy and Imaging of Cancer Cells

ARTICLE *in* ANALYTICAL CHEMISTRY · FEBRUARY 2014

Impact Factor: 5.64 · DOI: 10.1021/ac404201s · Source: PubMed

CITATIONS

15

READS

104

8 AUTHORS, INCLUDING:



[Chao Ma](#)

Northwest A & F University

12 PUBLICATIONS 22 CITATIONS

[SEE PROFILE](#)



[Rui Zhang](#)

Texas A&M University

11 PUBLICATIONS 62 CITATIONS

[SEE PROFILE](#)



[Saeed Elraey](#)

Northwest A & F University

2 PUBLICATIONS 15 CITATIONS

[SEE PROFILE](#)



[Mahmoud Abdelaal](#)

Northwest A & F University

3 PUBLICATIONS 16 CITATIONS

[SEE PROFILE](#)

Small Molecule-Initiated Light-Activated Semiconducting Polymer Dots: An Integrated Nanoplatform for Targeted Photodynamic Therapy and Imaging of Cancer Cells

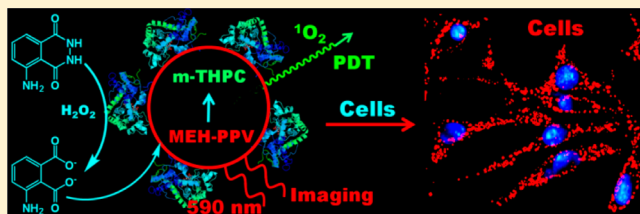
Yanrong Zhang,^{†,‡} Long Pang,^{‡,§} Chao Ma,[‡] Qin Tu,[†] Rui Zhang,[§] Elray Saeed,[‡] Abd Elaal Mahmoud,[‡] and Jinyi Wang^{*,†,‡}

[†]College of Science and [‡]College of Veterinary Medicine, Northwest A&F University, Yangling, Shaanxi 712100, P. R. China

[§]Department of Chemistry & Biochemistry, Florida International University, Miami, Florida 33199, United States

Supporting Information

ABSTRACT: Photodynamic therapy (PDT) is a noninvasive and light-activated method for cancer treatment. Two of the vital parameters that govern the efficiency of PDT are the light irradiation to the photosensitizer and visual detection of the selective accumulation of the photosensitizer in malignant cells. Herein, we prepared an integrated nanoplatform for targeted PDT and imaging of cancer cells using folic acid and horseradish peroxidase (HRP)-bifunctionalized semiconducting polymer dots (FH-Pdots). In the FH-Pdots, meta-tetra(hydroxyphenyl)-chlorin (m-THPC) was used as photosensitizer to produce cytotoxic reactive oxygen species (ROS); fluorescent semiconducting polymer poly[2-methoxy-5-((2-ethylhexyl)oxy)-*p*-phenylenevinylene] was used as light antenna and hydrophobic matrix for incorporating m-THPC, and amphiphilic Janus dendrimer was used as a surface functionalization agent to conjugate HRP and aminated folic acid onto the surface of FH-Pdots. Results indicated that the doped m-THPC can be simultaneously excited by the on-site luminol–H₂O₂–HRP chemiluminescence system through two paths. One is directly through CRET and subsequent fluorescence resonance energy transfer. In vitro PDT and specificity studies of FH-Pdots using a standard transcriptional and translational assay against MCF-7 breast cancer cells, C6 glioma cells, and NIH 3T3 fibroblast cells demonstrated that cell viability decreased with increasing concentration of FH-Pdots. At the same concentration of FH-Pdots, the decrease in cell viability was positively relevant with increasing folate receptor expression. Results from in vitro fluorescence imaging exhibited that more FH-Pdots were internalized by cancerous MCF-7 and C6 cells than by noncancerous NIH 3T3 cells. All the results demonstrate that the designed semiconducting FH-Pdots can be used as an integrated nanoplatform for targeted PDT and on-site imaging of cancer cells.



Photodynamic therapy (PDT) as an emerging therapeutic modality for cancer has gained increasing attention recently.^{1,2} Compared with conventional approaches, such as chemotherapy, surgery, and radiotherapy, PDT is noninvasive and can achieve equivalent or high efficacy with greatly reduced morbidity and disfigurement.³ In PDT, a photosensitive drug (photosensitizer) is activated by proper light and releases cytotoxic reactive oxygen species (ROS) to eradicate cancer cells.⁴ Therefore, two of the vital parameters that govern the efficiency of PDT are the light irradiation to photosensitizer and the visual detection of the selective accumulation of the photosensitizer in malignant cells. Photosensitizers generally have a strong absorption at approximately 400 nm (Soret band) and a weak absorption at approximately 600–800 nm (Q-band).⁵ The excitation of photosensitizers at the Soret band is much more efficient than that at the Q-band. Therefore, photosensitizers are commonly excited by visible or UV light, which greatly limits tissue penetration depth because of the light absorption and scattering by biological tissues and finally results in low and even ineffective therapeutic effects.⁶ To

resolve this limitation, many efforts have been devoted to design new photosensitizers with high cross section of two-photon absorption.⁷ For example, photosensitizers are conjugated with other light antenna molecules to activate photosensitizers through fluorescence resonance energy transfer (FRET).⁸ Alternatively, photosensitizers are conjugated with upconversion nanoparticles (UCNPs) to absorb more than two low-energy pump photons in the near-infrared region in a cascade manner and convert them into higher-energy photons in the visible region.^{9,10} Although these designs, especially the use of infrared light, can reduce the shortcoming of low tissue penetration, the development of photosensitizers with highly efficient absorption of infrared light is challenging. In addition, the requirement of outer light source always limits the effective application of these designs in PDT. Thus, the development of a novel PDT system that has an independent

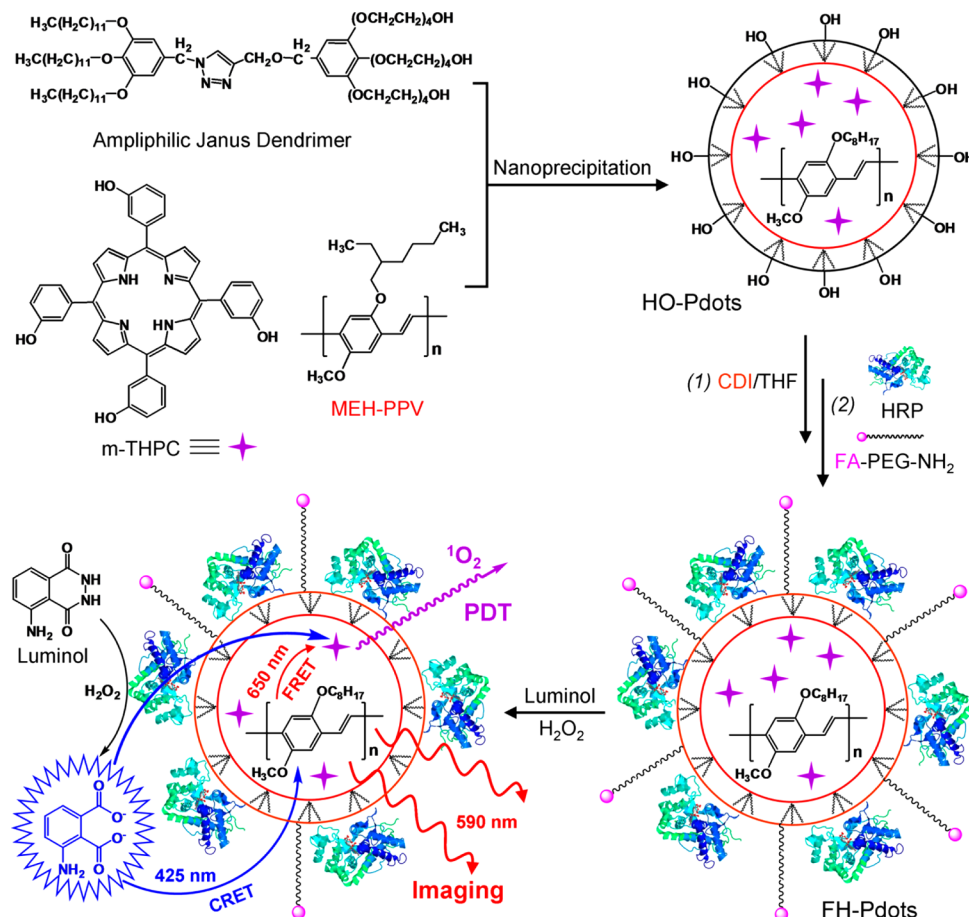
Received: December 18, 2013

Accepted: February 19, 2014

Published: February 19, 2014



Scheme 1. Schematic Presentation of the Preparation of FH-Pdots and the Mechanism of ROS Generation for PDT and Fluorescence Imaging upon the Addition of Chemiluminescence Substrates



internal light source can provide a new therapy modality for various diseases.

Cheミluminescence resonance energy transfer (CRET) or bioluminescence resonance energy transfer (BRET), which involves nonradiative transfer of energy from a chemiluminescent or bioluminescent donor to a suitable acceptor molecule, has been applied in biological imaging and sensing without the use of an external light source.^{11–14} However, to date, only two studies have used BRET or CRET for PDT system construction.^{15,16} Lai et al. constructed a PDT system by using *Renilla luciferase* 8-immobilized quantum dots (QDs) as the internal light source to excite photosensitizers via BRET.¹⁵ Wang et al. used the luminol–H₂O₂–horseradish peroxidase (HRP) chemiluminescence system to excite oligo (*p*-phenylene vinylene) through CRET.¹⁶ The two studies have greatly exhibited the potential of utilizing chemiluminescence or bioluminescence as the excitation light source for PDT. However, the study of chemiluminescence or bioluminescence for PDT system remains in its infant stage. QDs have several advantages, such as narrow emission, broad absorbance, bright luminescence, and good photostability. However, their applications are limited by their inherent disadvantages, such as blinking behavior and cytotoxicity. In addition, in the current studies, the luminescence unit and photosensitizer are in their respective microenvironments or are connected by electrostatic interaction, which might reduce the efficiency of energy transfer since energy transfer efficiency is inversely proportional to the

sixth power of the distance between the donor and the acceptor.¹⁷

Semiconducting polymer dots (Pdots), a new class of ultrabright fluorescent probes, have recently drawn special attention because of their several important characteristics for biological imaging and biosensing studies, such as their high brightness, fast emission rate, excellent photostability, and nonblinking behavior.^{18–21} More importantly, previous studies have demonstrated that Pdots are extremely biocompatible compared with the potential toxicity of QDs and UCNPs. Although Pdots are usually hydrophobic and difficult to be functionalized with other desired molecules, coprecipitating semiconducting polymers with amphiphilic molecules can make Pdots hydrophilic and be easily modified with various molecules (e.g., biological targeting entities and proteins).²¹ All these properties make Pdots the ideal matrix and light antenna for entrapping hydrophobic molecules (e.g., photosensitizers) and for transferring their emission light to hydrophobic molecules through resonance energy transfer.

On the basis of the analysis above, herein, we constructed a small molecule-initiated light-activated semiconducting Pdot system for targeted PDT and on-site imaging of cancer cells (Scheme 1). First, we coprecipitated amphiphilic Janus dendrimer and photosensitizer meta-tetra(hydroxyphenyl)-chlorin (m-THPC) with semiconducting polymer poly[2-methoxy-5-((2-ethylhexyl)oxy)-*p*-phenylenevinylene] (MEH-PPV) to prepare hydroxyl-terminated photosensitizer-doped Pdots (HO-Pdots). Amphiphilic Janus dendrimer is chosen

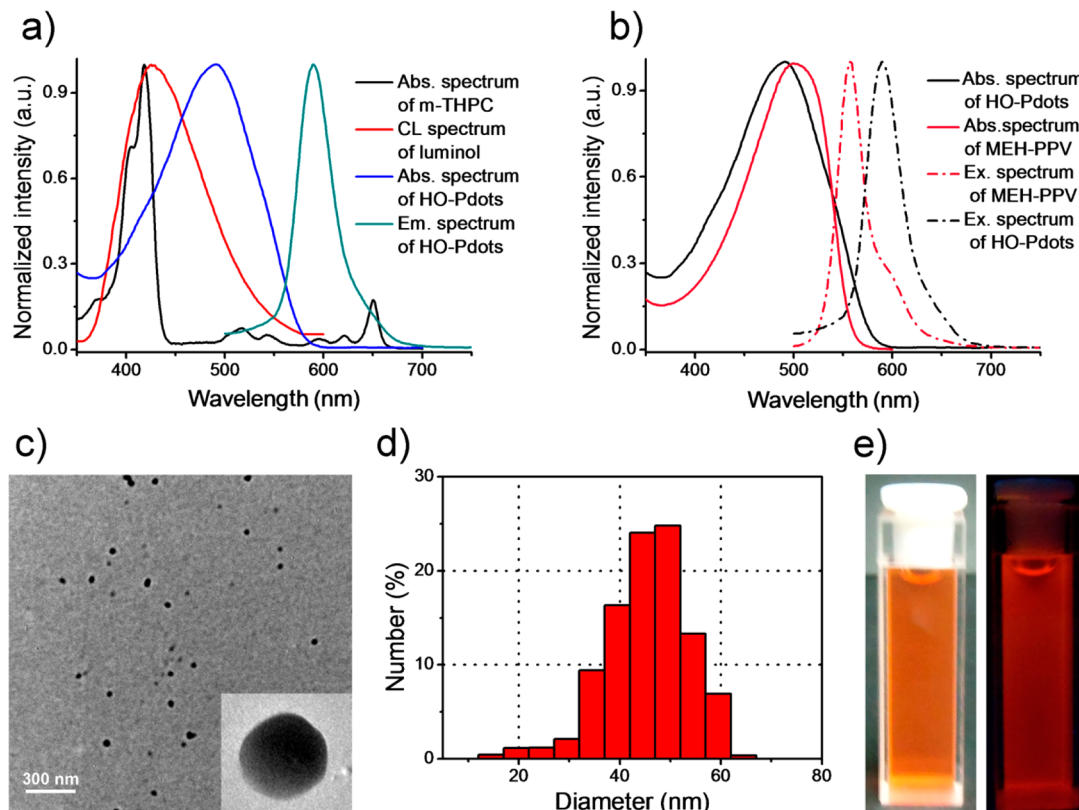


Figure 1. (a) Normalized absorption spectra of m-THPC and HO-Pdots and emission spectra of HO-Pdots and the chemiluminescence (CL) of luminol. (b) Normalized absorption and fluorescence spectra of HO-Pdots and parent polymer MEH-PPV. (c) A representative TEM image of HO-Pdots; inset shows the enlarged view of a single HO-Pdot. (d) Hydrodynamic diameter of HO-Pdots measured by DLS. (e) Photographs of HO-Pdot suspension under natural light (left) and 365 nm UV irradiation (right).

because it is a powerful amphiphile with greater versatility than simple lipids, surfactant, or block copolymers.^{22,23} In addition, the dendronized poly(ethylene glycol) moiety might effectively cover the inherent hydrophobic surface of native Pdots. Then, folic acid (FA) and HRP were covalently conjugated on the Pdots to obtain FA- and HRP-bifunctionalized Pdots (FH-Pdots). FA acts as the tumor-targeting ligand to improve the selectivity of Pdots for cancer cells, and HRP acts as the catalyst for the luminol–H₂O₂–HRP chemiluminescence system. Through two paths (one is directly through CRET and the other is through CRET and FRET successively), the main absorptions of m-THPC can be simultaneously excited to produce ROS for PDT without the use of an external light source. At the same time, the on-site fluorescence imaging of cells was also realized via the semiconducting Pdots. Relevant in vitro experiments against cancerous MCF-7 and C6 cells and noncancerous NIH 3T3 cells were performed to validate the design of this novel self-illuminating PDT system.

EXPERIMENTAL SECTION

Preparation of FH-Pdots. FH-Pdots were prepared by using a nanoprecipitation technique.^{21,24} For the detailed information, see Supporting Information.

Detection of ROS Generation. ROS produced by semiconducting Pdots were detected using 9,10-anthracenediylibis(methylene) dimalonic acid (ABDA)²⁵ and typical ROS emission at 1270 nm.¹⁰ The sample solution was prepared by mixing 2.5 mL of Pdot dispersion and 25 μL of ABDA solution (2 mg/mL). The light beam from a xenon lamp at 420 nm was focused onto a quartz cuvette (1 cm path

length) containing the sample solution. The UV–vis absorption spectra were measured by using a UV–vis spectrophotometer (Thermo Electron Corporation, Nicolet 300). To detect the ROS photoluminescence, the Pdots without or with m-THPC were dispersed in D₂O²⁶ and then saturated with oxygen gas for 30 min before experiment.¹⁰ An 850 nm long-pass filter was placed before the detector. The spectra were recorded using a combined steady-state and lifetime fluorescence spectrometer (Edinburgh Instruments, Flsp920).

Cell Culture and Imaging. C6 glioma cells and NIH 3T3 fibroblasts cells were routinely cultured with Dulbecco's modified Eagle's medium supplemented with 10% fetal bovine serum, 100 U/mL penicillin, and 100 μg/mL streptomycin at 37 °C in a 5% CO₂ atmosphere. MCF-7 breast cancer cells were cultured in Roswell Park Memorial Institute medium 1640 supplemented with 10% fetal bovine serum at 37 °C in a humidified and 5% CO₂ incubator. For imaging, MCF-7, C6, and NIH 3T3 cells at a density of 5 × 10⁴ cells/mL were cultivated for 24 h on coverslips in 12-well culture plates (1 mL/well). Then, suspensions of FH-Pdots were added (0.5 mL/well, 5 μg/mL) and incubated for 6 h. The cells were then washed thrice with phosphate-buffered saline (PBS, pH 7.4) and fixed using 4% (v/v) paraformaldehyde aqueous solution. After that, the cells were fixed for 20 min at room temperature and rinsed with PBS, and then, 0.5 μg/mL Hoechst 33258 in PBS was added to stain the nuclei for 10 min. The cell images were obtained under an inverted microscope (Olympus, CKX41).

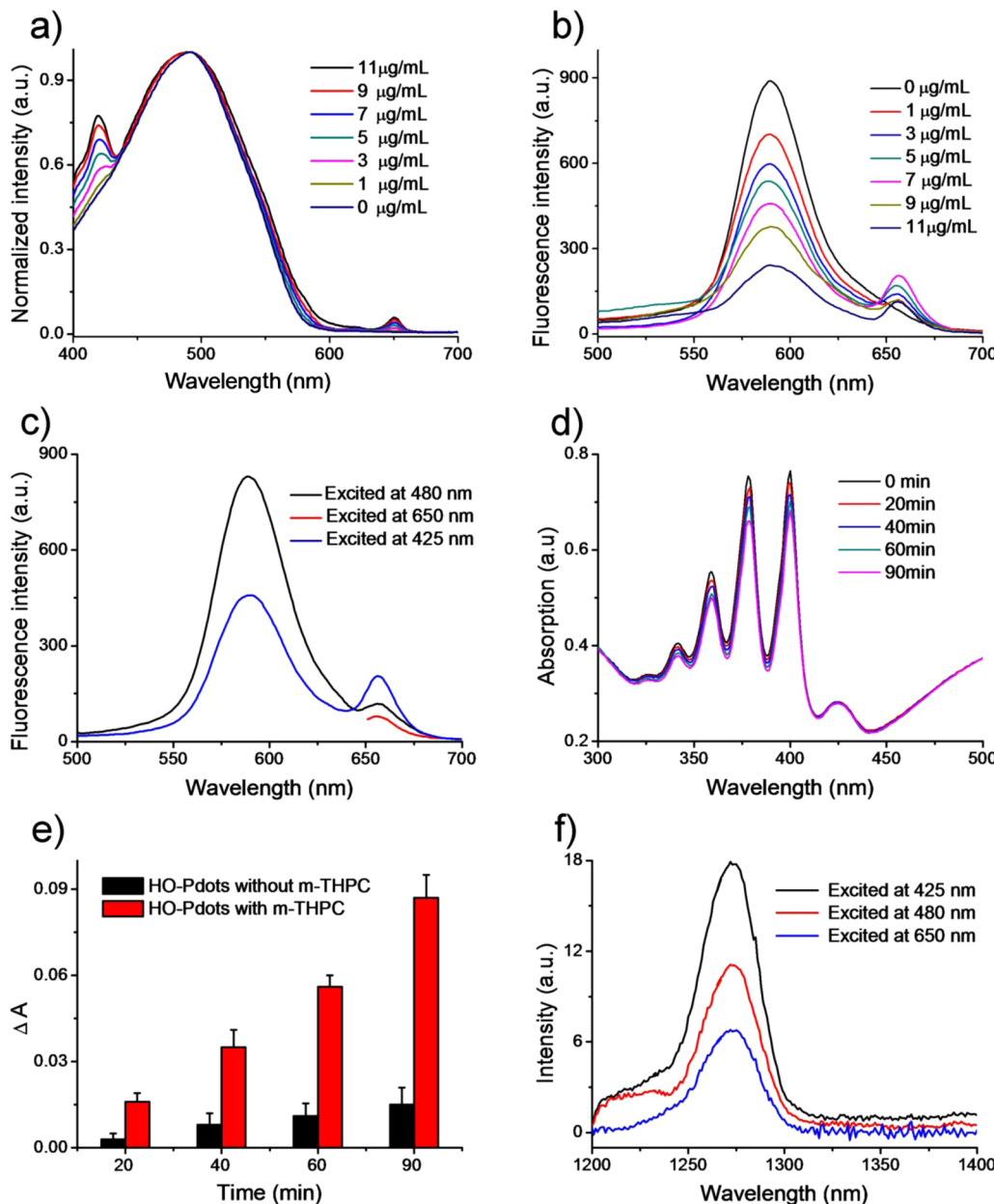


Figure 2. (a) UV-vis absorption and (b) fluorescence spectra of HO-Pdots with indicated concentration of m-THPC. (c) Emission spectra of HO-Pdots excited at 480, 650, and 425 nm, respectively. (d) Absorption spectra of ABDA in the presence of m-THPC containing HO-Pdots under different irradiation times at 425 nm. (e) Comparison of the absorbance change of ABDA by HO-Pdots with or without m-THPC doped as a function of irradiation time. (f) Emission spectra of ROS generated by HO-Pdots excited at 480, 650, and 425 nm, respectively.

RESULTS AND DISCUSSION

Design of the Multifunctional Semiconducting Polymer Dots. In the current study, m-THPC, a second-generation photosensitive drug for cancer treatment, was chosen as the photosensitizer to produce ROS when excited by appropriate light. m-THPC has two main absorptions at 420 and 650 nm (Figure 1a). However, it was always excited only at 650 nm in outer light source-based studies because this wavelength belongs to the near-infrared region.^{27,28} It should be noted that the extinction coefficient of m-THPC at 420 nm is approximately 5-fold higher than that at 650 nm (Figure S2 in Supporting Information). Therefore, exciting m-THPC simultaneously at the two wavelengths by a single-light irradiation would be more effective. The semiconducting polymer MEH-PPV was employed as the doping host because it is

commercially available and because Pdots formed by MEH-PPV have broad absorption (400 to 550 nm; Max. 492 nm) and emission (550 to 700 nm; Max. 590 nm). HRP was chosen as a model enzyme because the luminol–H₂O₂ chemiluminescence catalyzed by HRP is one of most sensitive chemiluminescence reactions that has been widely used in biological assays, emitting blue light (350 to 550 nm) with the maximum at 425 nm.^{13,14,16} As shown in Figure 1a, the absorption of m-THPC at 420 nm overlaps well with the emission band of luminol (350 to 550 nm), the absorption of m-THPC at 650 nm is included in the emission band of MEH-PPV Pdots (550 to 700 nm), and the absorption band of MEH-PPV Pdots (400 to 550 nm) also partially overlaps with the emission band of luminol (350 to 550 nm); all of these meet the spectral overlap requirement for resonance energy transfer as the donor–acceptor pair.

Therefore, in the proposed PDT system, the two main absorptions of m-THPC can be excited simultaneously through two different paths. One is directly through CRET between the luminol–H₂O₂–HRP chemiluminescence system and m-THPC, and the other is through the CRET between the chemiluminescence system and MEH-PPV and subsequently through the FRET between MEH-PPV and m-THPC. Meanwhile, the on-site fluorescence imaging of cells can be also realized via the emission of the MEH-PPV semiconducting Pdots.

Preparation and Characterization of HO-Pdots. To preliminarily explore the feasibility of the above-mentioned idea, we first prepared HO-Pdots using a nanoprecipitation technique.^{21,24} For the detailed information, see Supporting Information. The rapid addition of the tetrahydrofuran (THF) solution of MEH-PPV, m-THPC, and amphiphilic Janus dendrimer to deionized water under vigorous sonication leads to the collapse of the polymer chains because of the sudden change in their microatmosphere, which results in the formation of HO-Pdots as well as the simultaneous entrapment of hydrophobic m-THPC molecules inside the hydrophobic core of the HO-Pdots.^{20,24} In this process, the morphology and size of HO-Pdots can be affected by some key parameters, including the volume ratio of THF to water, the molar ratio of amphiphilic Janus dendrimer to MEH-PPV, and the power and time of sonication. Small particles benefit cellular uptake and distribution, provide a large surface-to-volume ratio, and reduce the distance over which chemiluminescence is relayed to the interior of the Pdots.²⁰ After numerous optimization experiments, we found that suitable Pdots formed under the following parameters: THF-to-water volume ratio of 1:3, amphiphilic Janus dendrimer-to-MEH-PPV molar ratio of 10:1, and vigorous sonication (520 W) time of 60 s. The average size of the resulting HO-Pdots was determined to be ~45 nm (Figure 1c) in diameter from transmission electron microscopy (TEM) measurement and to be ~50 nm (Figure 1d) in diameter from dynamic light scattering (DLS). The difference in diameter is likely due to TEM measuring the Pdots diameter after they had been dried and shrunk on the carbon-supported copper grid surface, while DLS determined it in solution where they were hydrated and thus in a more “swollen” state.²⁹ Absorption and fluorescence spectra (Figure 1b) show that the photophysical properties of the parent polymer MEH-PPV in THF differed from those of the HO-Pdots in water. The blue-shifted absorption (~8 nm) and the red-shifted emission (~33 nm) prove the formation of HO-Pdots.³⁰ The aqueous suspension of the obtained HO-Pdots is stable and clear (not turbid) and exhibits strong red fluorescence under UV (365 nm) illumination (Figure 1e).

We then optimized the amount of m-THPC doped to minimize the self-quenching effect among the encapsulated m-THPC molecules, because aggregated photosensitizer molecules could result in less photoactivation and less ROS in solution.² Various concentrations of m-THPC were respectively mixed with constant MEH-PPV and amphiphilic Janus dendrimer THF solution to prepare HO-Pdots. In the UV-vis absorption spectra (Figure 2a) of HO-Pdots containing different amounts of m-THPC, two dominant absorption peaks appeared at 420 and 492 nm, and a weak absorption peak appeared at 650 nm. The absorbance at 420 and 650 nm increased as the concentration of m-THPC increased. These phenomena indicate that the two hydrophobic molecules MEH-PPV and m-THPC were successfully incorporated into

the HO-Pdots. Figure 2b is the fluorescence spectra of HO-Pdots containing different amounts of m-THPC. The fluorescence intensity at 590 nm decreased with an increasing amount of doped m-THPC. This result might be caused by the FRET between MEH-PPV and m-THPC. To confirm this point, the fluorescence lifetime of HO-Pdots with and without m-THPC was recorded at 590 nm (Figure S3 in Supporting Information). The fluorescence lifetime of HO-Pdots with m-THPC decreased from 490 to 370 ps, indicating the existence of FRET from MEH-PPV to m-THPC. In addition, the fluorescence intensity of m-THPC at 656 nm was modulated by the amount of m-THPC doped in the nanoparticle matrix. High m-THPC concentrations decreased the m-THPC fluorescence intensity because of self-quenching of m-THPC. The optimal concentration of m-THPC was 7 µg/mL and was used in the subsequent experiments.

To verify whether or not m-THPC can be simultaneously excited by CRET and CRET-to-FRET in the proposed PDT nanosystem, m-THPC containing HO-Pdots were excited respectively at 425, 480, and 650 nm. The excitation light of 425 nm was selected because it is the maximum emission wavelength of the luminol chemiluminescence and because it is close to the maximum absorption of m-THPC at 420 nm. In addition, it is located in the absorption band of MEH-PPV (400 to 550 nm). Thus, it can simultaneously excite m-THPC and MEH-PPV. The reason for the use of 480 nm is that it can only excite MEH-PPV. The emission of MEH-PPV can subsequently excite the other maximum absorption of m-THPC at 650 nm. As a control, the 650 nm maximum absorption wavelength of m-THPC was also utilized. It is obvious that the fluorescence intensity of m-THPC excited at 480 nm was approximately 1.5-fold higher than that excited at 650 nm (Figure 2c). This amplification can be attributed to FRET from the semiconducting polymer MEH-PPV.³¹ Similarly, when the HO-Pdots were excited at 425 nm, the fluorescence intensity of m-THPC was much higher than that excited at 480 nm because of the joint action of direct photoexcitation and FRET. Combining the fluorescence intensity change of MEH-PPV with the increasing amount of m-THPC and the fluorescence lifetime analysis of HO-Pdots, it is now not difficult to conclude that the m-THPC doped in Pdots can be simultaneously excited through CRET and CRET-to-FRET under 425 nm light irradiation.

The ability of m-THPC to produce ROS after excitation at 425 nm was evaluated by the oxidation reaction of ABDA in the presence of Pdots. ABDA is a sensitive ROS detection reagent. The absorbance of ABDA at 380 nm obviously decreased upon oxidation by ROS to convert to an endoperoxide.²⁵ Figure 2d shows the oxidation of ABDA in the presence of HO-Pdots under irradiation at 425 nm. During this test, HO-Pdots without m-THPC were employed as control. As shown in Figure 2e, the absorbance of ABDA at 380 nm decreased continuously over the course of irradiation but did not change in the control.³² Direct ROS monitoring by its characteristic phosphorescence (Figure 2f) showed that the typical ROS emission at 1270 nm¹⁰ can be clearly observed under excitation at 425 nm. In addition, the ROS emission can also be observed under excitation at 480 and 650 nm. The ratio of ROS emission intensity excited at 425, 480, and 650 nm was consistent with the ratio of m-THPC emission intensity excited at the same wavelengths (Figure 2c). These results demonstrate that m-THPC incorporated in the HO-Pdots can produce ROS

through simultaneous CRET and CRET-to-FRET under 425 nm light irradiation.

Preparation and Characterization of FH-Pdots. After obtaining the pleasing results above, we fabricated FH-Pdots. FA-PEG₂₀₀₀-NH₂ and HRP were conjugated onto the surface of Pdots through stable urethane linkages^{21,33} between the N,N'-carbonyldiimidazole (CDI)-activated hydroxyl groups and the terminal amino groups of HRP or FA-PEG₂₀₀₀-NH₂ (Scheme 1). The obtained FH-Pdots were further purified through ultrafiltration membrane (MWCO 100 kDa) to remove the uncoupled HRP, FA-PEG₂₀₀₀-NH₂, and excess CDI. Compared with HO-Pdots, FH-Pdots showed no obvious changes in morphology and size in the TEM images. However, DLS analysis revealed that the diameter of FH-Pdots increased from 22 to 26 nm (Figure S4 in Supporting Information). The possible reason may be that the TEM measurement corresponded to the diameter of the semiconducting polymer core because the poly(ethylene glycol) has poor contrast due to low electron density^{34,35} and that the DLS measurement corresponded to the mean hydrodynamic diameter of Pdots in water. The 11 to 13 nm increase in the radius is consistent with the length of the poly(ethylene glycol) moiety in the FA-PEG-NH₂.³⁶ The hydrodynamic diameter of HRP was estimated using spherical approximation to be 3.5 nm,³⁷ which is shorter than the length of the poly(ethylene glycol) chain. Therefore, the FA conjugated on the FH-Pdots can be easily connected with folate receptors on the cell membrane for targeted PDT and imaging.

To prove that the luminol-H₂O₂-HRP chemiluminescence system can also illuminate the FH-Pdots as an internal light source, the fluorescence properties of FH-Pdots without and with m-THPC were studied in the presence of chemiluminescence substrates. Figure 3a shows the fluorescence spectra of FH-Pdots without m-THPC, which shows two obvious emissions at 425 and 590 nm. Their fluorescence intensity gradually decreased as time was prolonged. These results indicated that HRP successfully catalyzed the chemiluminescence system, which subsequently excited the semiconducting polymer MEH-PPV through CRET. It is worth mentioning that CRET occurs only when the distance between the donor and acceptor is less than 10 nm.²⁴ To create such a CRET response, the excitation-state products of the HRP-catalyzed lunimol oxidation reaction must be diffused to FH-Pdots before they decay to their stable species.³⁸ Indeed, mixing the same amount of HRP as that conjugated on the FH-Pdots with no m-THPC contained HO-Pdots resulted in a weaker emission intensity at 590 nm compared with no m-THPC contained FH-Pdots (Figure S6 in Supporting Information). This observation proved that HRP was covalently conjugated on the FH-Pdots and highlighted that the CRET was the main mechanism to illuminate FH-Pdots. When chemiluminescence substrates were added to the m-THPC containing FH-Pdots, a new emission at 656 nm appeared (Figure 3b). Combining the previous single-light irradiation experiments, we can conclude that the constructed internal light source can successfully excite the m-THPC-doped Pdots to produce ROS via CRET and CRET-to-FRET upon the addition of chemiluminescence substrates.

Photodynamic Therapy and Imaging of Cancer Cells. The biocompatibility of materials is preliminary and central for its further biomedical application.^{18–21} The cytotoxicity of FH-Pdots was evaluated by monitoring the metabolic viability of cells after incubation with FH-Pdots through a standard MTT assay without adding the chemiluminescence substrates. For

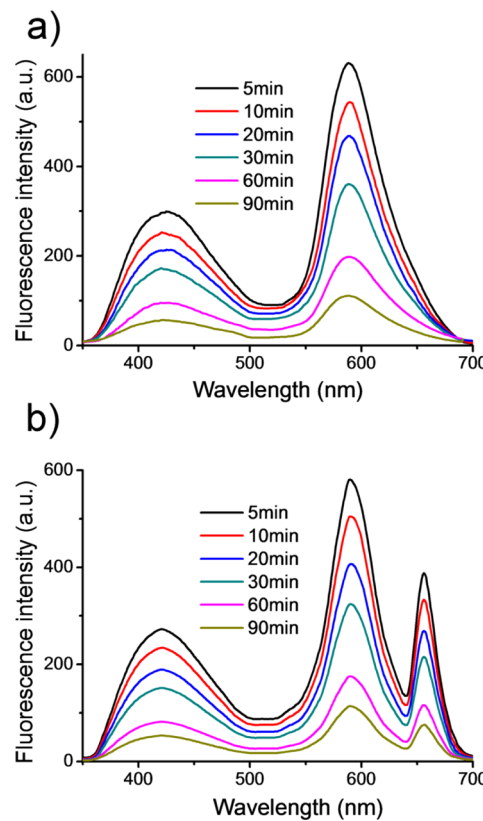


Figure 3. Chemiluminescence emission spectra of FH-Pdots (a) without and (b) with m-THPC doping.

comparisons, MCF-7 breast cancer cells were chosen for overexpressed folate receptors on its cell membrane; C6 glioma cells were chosen as the positive control, and NIH 3T3 fibroblast cells were chosen as the negative control. As shown in Figure S8a in Supporting Information, even when the concentration of FH-Pdots reached 10 μ g/mL (in terms of the concentration of m-THPC incorporated), they elicited no obvious cytotoxicity to cancerous and noncancerous cells in the dark. At the same time, two control experiments were conducted. One involved FH-Pdots without incorporating m-THPC (with the same concentration of MEH-PPV as above). The other involved the addition of chemiluminescence substrates to the FH-Pdots without m-THPC, which has almost the same cytotoxicity as that caused by the chemiluminescence substrates (Figure S7 in Supporting Information). These results demonstrated that FH-Pdots could be utilized in biorelated fields, which maybe be contributed to the fact that the introduction of the biocompatible dendrimer poly (ethylene glycol) moiety on the surface of FH-Pdots effectively prevents FH-Pdot aggregation on the cell surface.^{21,34}

Then, the photodynamic effect and targeting capability of FH-Pdots were further evaluated by incubating different concentrations of FH-Pdots with cancerous (MCF-7 and C6) and noncancerous (NIH 3T3) cells in the presence of chemiluminescence substrates. The cell viability was also determined by the MTT assay (Figure S8b in Supporting Information). The cytotoxicity became more prominent as the concentration of FH-Pdots increased. When the concentration was 10 μ g/mL, 72%, 32%, and 17% cell viabilities were observed for the NIH 3T3, C6, and MCF-7 cells, respectively.

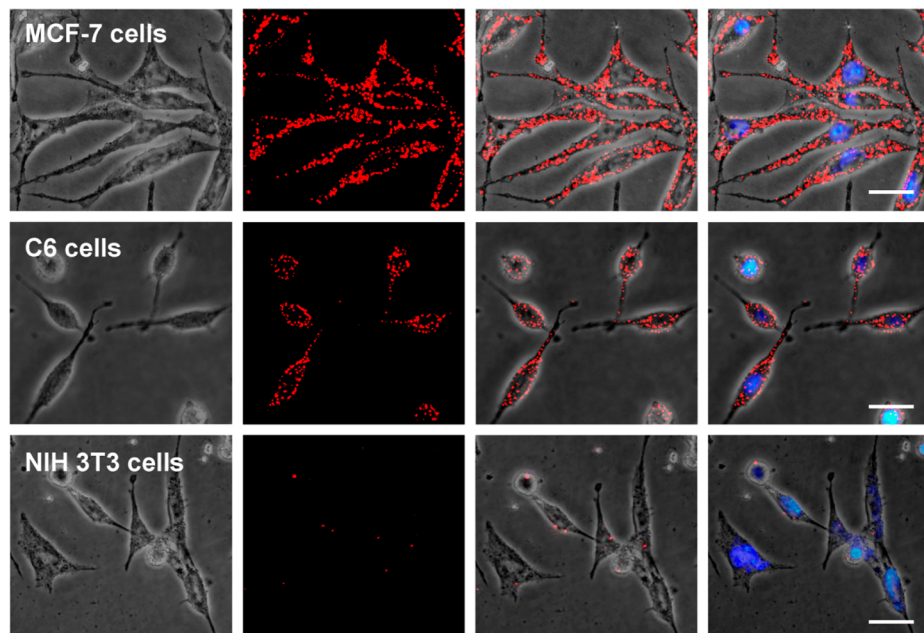


Figure 4. Phase contrast bright-field and fluorescence images of cancerous MCF-7 and C6 cells and noncancerous NIH 3T3 cells incubated with FH-Pdots for 6 h. From left to right, phase contrast bright-field image; fluorescence image; merged image of phase contrast bright-field and fluorescence images; merged image of phase contrast bright-field, fluorescence, and Hoechst 33258-stained images. Scale bar: 20 μm .

However, without adding the chemiluminescence substrates, >95% cell viability was observed for the three cell lines at 10 $\mu\text{g}/\text{mL}$ FH-Pdots. This dramatic difference shows that the ROS cytotoxicity of FH-Pdots can be activated by the chemiluminescence substrates. In addition, the difference in ROS cytotoxicity among the MCF-7, C6, and NIH 3T3 cells at the same FH-Pdot concentration demonstrates that FH-Pdots have excellent targeting capability because of the introduction of FA on the surface of FH-Pdots.

To visually observe the MTT assay results, the fluorescence imaging of the cells was also recorded after culture with FH-Pdots for 6 h. The cell nuclei were stained with Hoechst 33258. Pdots possess high inertia in the presence of ROS compared with QDs and common organic dyes.³⁹ Therefore, the fluorescence intensity of Pdots is stable and suitable for cell imaging at the atmosphere of ROS. As shown in Figure 4, red fluorescence from MEH-PP Pdots was mainly located in the cytoplasm and perinuclear regions. Compared with noncancerous NIH 3T3 cells, cancerous MCF-7 and C6 cells accumulated a large amount of FH-Pdots. Only a few FH-Pdots were taken up by noncancerous NIH 3T3 cells. This phenomenon illustrates that the endocytosis of FH-Pdots is mediated by folate receptors on the cell membrane and proves that FH-Pdots have excellent targeting capability for cancer cells because of their overexpressed folate receptors.

CONCLUSIONS

In this study, a smart chemiluminescence-initiated light-activated semiconducting Pdot for targeted PDT and imaging of cancer cells was constructed using the semiconducting polymer MEH-PPV. To realize targeted PDT and imaging of cancer cells, amphiphilic Janus dendrime was introduced in the semiconducting Pdots. Amphiphilic Janus dendrime not only effectively stabilizes Pdots but also serves as a functionalization agent for conjugating the tumor-targeting ligand FA and the chemiluminescence catalyst HRP onto the surface of Pdots. The fluorescent spectra demonstrated that the two main

absorptions (420 and 650 nm) of the photosensitizer m-THPC can be simultaneously excited through direct CRET and indirect CRET-to-FRET, which greatly improves ROS production efficiency. Meanwhile, the semiconducting Pdots can be illuminated for fluorescence imaging of cancer cells. The use of chemiluminescence as an internal light source addresses the limitation of the requirement of outer light source in a conventional PDT system. In vitro cytotoxicity assay of FH-Pdots showed that Pdots had excellent biocompatibility. Once FH-Pdots were activated by chemiluminescence, the cytotoxicity of FH-Pdots was higher for cells with more folate receptors. Similar to the cytotoxicity assays, fluorescence imaging revealed that more FH-Pdots were internalized by the cells with more folate receptors than those with less folate receptors. Although H_2O_2 , as a component of chemiluminescence substrates, has certain toxicity to cells, the present results demonstrate that the multifunctional semiconducting Pdots could act as a novel integrated nanoplatform for targeted PDT without the use of outer light source and for on-site fluorescence imaging of cancer cells. Relevant studies, such as the substitution of HRP with other enzymes to omit the use of H_2O_2 and the further applications in vivo of the FH-Pdots for targeted PDT and on-site imaging of tumor tissue, are under way in our laboratory.

ASSOCIATED CONTENT

Supporting Information

Materials and physical methods, synthesis, determination of extinction coefficients of m-THPC, measurement of fluorescence lifetime, preparation of HO-Pdots and FH-Pdots, spectral measurements of CRET from oxidized luminol to FH-Pdots, investigation of the particle size of FH-Pdots, effect of the incubation time on the amount of HRP conjugated on FH-Pdots, comparison of fluorescence spectra of FH-Pdots with that of the mixture of HO-Pdots and HRP, cellular viability, cytotoxicity of various concentrations of H_2O_2 and FH-Pdots to

cells, and ^1H - and ^{13}C -NMR spectra. This material is available free of charge via the Internet at <http://pubs.acs.org>.

AUTHOR INFORMATION

Corresponding Author

*Phone: +86-29-870 825 20. Fax: +86-29-870 825 20. E-mail: jywang@nwsuaf.edu.cn.

Author Contributions

[†]Y.Z. and L.P. contributed equally to this work.

Notes

The authors declare no competing financial interest.

ACKNOWLEDGMENTS

This study was supported by the National Natural Science Foundation of China (21375106 and 21175107), the Ministry of Education of the People's Republic of China (NCET-08-602 0464), the Fundamental Research Funds for the Central Universities (Z109021303), the Scientific Research Foundation for the Returned Overseas Chinese Scholars, the State Education Ministry, and the Northwest A&F University.

REFERENCES

- (1) Lincoln, R.; Kohler, L.; Monroe, S. M. A.; Stephenson, H.; Yin, M.; Thummel, R. P.; Mcfarland, S. A. *J. Am. Chem. Soc.* **2013**, *135*, 17161–17175.
- (2) Wieczorek, S.; Krause, E.; Hackbarth, S.; Röder, B.; Hirsch, A. K. H.; Börner, H. G. *J. Am. Chem. Soc.* **2013**, *135*, 1711–1714.
- (3) Hopper, C. *Lancet Oncol.* **2000**, *1*, 212–219.
- (4) Zhang, P.; Steelant, W.; Kumar, M.; Scholfield, M. *J. Am. Chem. Soc.* **2007**, *129*, 4526–4527.
- (5) Alexiades-Armenakas, M. *Clin. Dermatol.* **2006**, *24*, 16–25.
- (6) Zhao, H.; Doyle, T. C.; Coquoz, O.; Kalish, F.; Rice, B. W.; Contag, C. H. *J. Biomed. Opt.* **2005**, *10*, 041210.
- (7) Kuimova, M. K.; Collins, H. A.; Balazs, M.; Dahlstedt, E.; Levitt, J. A.; Sergent, N.; Suhling, K.; Drobizhev, M.; Makarov, N. S.; Rebane, A.; Anderson, H. L.; Phillips, D. *Org. Biomol. Chem.* **2009**, *7*, 889–896.
- (8) Samia, A. C. S.; Dayal, S.; Burda, C. *Photochem. Photobiol.* **2006**, *82*, 617–625.
- (9) Wang, C.; Tao, H. Q.; Cheng, L.; Liu, Z. *Biomaterials* **2011**, *32*, 6145–6154.
- (10) Liu, K.; Liu, X. M.; Zeng, Q. H.; Zhang, Y. L.; Tu, L. P.; Liu, T.; Kong, X. G.; Wang, Y. H.; Cao, F.; Lambrechts, S. A. G.; Aalders, M. C. G.; Zhang, H. *ACS Nano* **2012**, *6*, 4054–4062.
- (11) Yao, H. Q.; Zhang, Y.; Xiao, F.; Xia, Z. Y.; Rao, J. H. *Angew. Chem., Int. Ed.* **2007**, *46*, 4346–4349.
- (12) Wu, C.; Mino, K.; Akimoto, H.; Kawabata, M.; Nakamura, K.; Ozaki, M.; Ohmiya, Y. *Proc. Natl. Acad. Sci. U.S.A.* **2009**, *106*, 15599–15603.
- (13) Freeman, R.; Liu, X. Q.; Willner, I. *J. Am. Chem. Soc.* **2011**, *133*, 11597–11604.
- (14) Zhang, S. S.; Yan, Y. M.; Bi, S. *Anal. Chem.* **2009**, *81*, 8695–8701.
- (15) Hsu, C. Y.; Chen, C. W.; Yu, H. P.; Lin, Y. F.; Lai, P. S. *Biomaterials* **2013**, *34*, 1204–1212.
- (16) Yuan, H. X.; Chong, H.; Wang, B.; Zhu, C. L.; Liu, L. B.; Yang, Q.; Lv, F. T.; Wang, S. *J. Am. Chem. Soc.* **2012**, *134*, 13184–13187.
- (17) Ishida, Y.; Shimada, T.; Masui, D.; Tachibana, H.; Inoue, H.; Takagi, S. *J. Am. Chem. Soc.* **2011**, *133*, 14280–14286.
- (18) Wu, C. F.; Bull, B.; Szymanski, C.; Christensen, K.; McNeill, J. *ACS Nano* **2008**, *2*, 2415–2423.
- (19) Yu, J. B.; Wu, C. F.; Sahu, S. P.; Fernando, L. P.; Szymanski, C.; McNeill, J. *J. Am. Chem. Soc.* **2009**, *131*, 18410–18414.
- (20) Wu, C. F.; Bull, B.; Christensen, K.; McNeill, J. *Angew. Chem., Int. Ed.* **2009**, *48*, 2741–2745.
- (21) Koner, A. L.; Krndija, D.; Hou, Q.; Sherratt, D. J.; Howarth, M. *ACS Nano* **2013**, *7*, 1137–1144.
- (22) Percec, V.; Wilson, D. A.; Leowanawat, P.; Wilson, C. *J. Science* **2009**, *328*, 1009–1014.
- (23) Petkau, K.; KAESER, A.; Fischer, I.; Brunsved, L.; Schenning, A. P. H. *J. Am. Chem. Soc.* **2011**, *133*, 17063–17071.
- (24) Xiong, L. Q.; Shuhendler, A. J.; Rao, J. H. *Nat. Commun.* **2012**, *3*, 1193–1200.
- (25) Lindig, B. A.; Rodgers, M. A. J.; Schaap, A. P. *J. Am. Chem. Soc.* **1980**, *102*, 5590–5593.
- (26) Kuimova, M. K.; Yahioglu, G.; Ogilby, P. R. *J. Am. Chem. Soc.* **2009**, *131*, 332–340.
- (27) Jones, H. J.; Vernon, D. I.; Brown, S. B. *Br. J. Cancer* **2003**, *89*, 398–404.
- (28) Bourré, L.; Simonneaux, G.; Ferrand, Y.; Thibaut, S.; Lajat, Y.; Patrice, T. *J. Photochem. Photobiol. B* **2003**, *69*, 179–192.
- (29) Yu, J. B.; Wu, C. F.; Zhang, X. J.; Ye, F. M.; Gallina, M. E.; Rong, Y.; Wu, I. C.; Sun, W.; Chan, Y. H.; Chiu, D. T. *Adv. Mater.* **2012**, *24*, 3498–3504.
- (30) Wu, C. F.; Chiu, D. T. *Angew. Chem., Int. Ed.* **2013**, *52*, 3086–3109.
- (31) Shen, X. Q.; Li, L.; Wu, H.; Yao, S. Q.; Xu, Q. H. *Nanoscale* **2011**, *3*, 5140–5146.
- (32) Zhao, T. T.; Wu, H.; Yao, S. Q.; Xu, Q. H.; Xu, G. Q. *Langmuir* **2010**, *26*, 14937–14942.
- (33) Pathak, S.; Choi, S. K.; Arnhem, N.; Thompson, M. E. *J. Am. Chem. Soc.* **2001**, *123*, 4103–4104.
- (34) Howes, P.; Green, M.; Levitt, J.; Suhling, K.; Hughes, M. *J. Am. Chem. Soc.* **2010**, *132*, 3989–3996.
- (35) Liu, Y.; Yehl, K.; Narui, Y.; Salaita, K. *J. Am. Chem. Soc.* **2013**, *135*, 5320–5323.
- (36) Wang, S. J.; Huang, P.; Nie, L. M.; Xing, R. J.; Liu, D. B.; Wang, Z.; Lin, J.; Chen, S. H.; Niu, G.; Lu, G. M.; Chen, X. Y. *Adv. Mater.* **2013**, *25*, 3055–3061.
- (37) Onda, M.; Lvov, Y.; Ariga, K.; Kunitake, T. *Biotechnol. Bioeng.* **1996**, *51*, 163–167.
- (38) Du, J. J.; Yu, C. M.; Pan, D. C.; Li, J. M.; Chen, W.; Yan, M.; Segura, T.; Lu, Y. F. *J. Am. Chem. Soc.* **2010**, *132*, 12780–12781.
- (39) Pu, K. Y.; Shuhendler, A. J.; Rao, J. H. *Angew. Chem., Int. Ed.* **2013**, *52*, 10325–10329.